Incubation Experiments, Observations and Modeling Highlight the Key Role of Dimethylmercury on Seawater Methylmercury Distributions

Alina Kleindienst[1*], Emmanuel Tessier[1], Johannes Bieser[2], Natalia Torres-Rodríguez[3], Océane Asensio[1], Aurélie Dufour[3], Claire Gassie[1], Lars-Eric Heimbürger-Boavida[3], Rémy Guyoneaud[1], David Amouroux[1*]

*E-mail: a.kleindienst@univ-pau.fr, david.amouroux@univ-pau.fr

[1]Université de Pau et des Pays de l'Adour, E2S-UPPA, CNRS, IPREM, Institut des Sciences Analytiques et de Physico-chimie pour l'Environnement et les Matériaux, Pau, France

[2]Institute of Coastal Systems – Analysis and Modeling, Helmholtz-Zentrum Hereon, Max-Planck-Str. 1, 21502 Geesthacht, Germany

[3]Aix Marseille Université, CNRS, IRD, Univ. Toulon, Mediterranean Institute of Oceanography (MIO), 13288 Marseille, France

Key words:

Methylated Mercury, Enriched Stable Isotopic Tracer Experiments, Atlantic Ocean, Mediterranean Sea, 1D Water Column Model, Marine Hg Cycle

Short Synopsis Statement:

Explaining ambient methylated mercury concentrations in seawater requires considering both dimethylmercury and monomethylmercury, along with their formation rates and stability.

Abstract

The origin of the bioaccumulative neurotoxin methylmercury (MeHg) in the ocean remains elusive. The current paradigm suggests that microbial methylation of inorganic Hg within the oceanic water column produces monomethylmercury (MMHg) and potentially dimethylmercury (DMHg). Reaction rates and main drivers governing MeHg levels (sum of MMHg and DMHg) are poorly constrained. We conducted ambient Hg species measurements and enriched isotopic tracer experiments in waters of two contrasting marine environments, the oligotrophic Mediterranean Sea (MED) and the mesotrophic Atlantic Ocean (ATL). Maximum subsurface MeHg levels were ~2 times higher in the MED compared to the ATL, essentially driven by higher DMHg concentrations (0.45 ± 0.06 vs 0.16 ± 0.02 pM). Methylation was only detectable in unfiltered subsurface waters and presumably biotically driven. The highest methylation rate (MMHg to DMHg) was observed in subsurface MED waters while reduction and demethylation rates were highest in surface waters of both environments. Experimental reaction rates and the potential microbial activity (based on 16S rDNA) aligned with ambient Hg species distributions.

Assuming high DMHg stability and applying our fast experimental DMHg formation rates, a newly developed 1D water column model (MED) successfully reproduced MeHg species distribution, suggesting DMHg plays a key role in the global marine Hg cycle.

1. Introduction

Monomethylmercury (MMHg) is of global concern due to the capacity of this neurotoxin to biomagnify across trophic levels [1]. The primary exposure pathway to MMHg for humans is the consumption of marine fish [2]. The Minamata Convention aims to reduce human exposure to Hg, by reducing anthropogenic Hg emissions, with substantial progress made since its ratification [3]. Mercury remains of concern since anthropogenic activities have led to an approximately threefold increase of oceanic surface Hg concentrations compared to pre-anthropogenic levels [4].

Once Hg has entered the ocean it can undergo a series of abiotic and biotic transformations (e.g. methylation, demethylation, reduction, oxidation) [5]. The main Hg species found in the ocean are monomethylmercury (MMHg), dimethyl Hg (DMHg), elemental Hg (Hg(0)), and inorganic mercuric Hg (Hg(II))[6]. Due to analytical constraints operationally defined Hg species such as methylated mercury (MeHg) as the sum of MMHg and DMHg and dissolved gaseous Hg (DGM) the sum of Hg(0) and DMHg are commonly reported [7].

Despite considerable efforts, a lack of understanding persists on Hg transformation pathways likely governing ambient Hg species concentrations. The limitations of our current understanding of MeHg cycling in the ocean is exemplified by the limited reproducibility of MeHg observations in oceanic waters by coupled biogeochemical models [8,9]. The prevailing scientific consensus agrees on biotic *in situ* Hg methylation [10,11] as the major source of MeHg in oceanic waters, with its distribution often closely linked to microbial organic matter degradation [12–14].

The importance of anaerobic microorganisms (e.g. sulfate-reducing bacteria, iron-reducing bacteria, methanogenic archaea) in mediating methylation is well known in anoxic environments, with the *hgcAB* genes encoding for Hg methylation [15]. Microbes thriving in oxic marine waters bear similar Hg transformation genes but their importance in Hg methylation is still debated [16–18]. Incubation experiments evidence the methylation of Hg(II) in oxic marine waters [10,11]. The cycling of DMHg in seawater is less understood, but it appears to be connected to the formation and decomposition of MMHg [10,19–22].

68 The *mer operon*, broadly distributed among prokaryotes [23–25], encodes for enzymes mediating
69 reduction (MerA) and demethylation (MerB). The presence and activity of the *mer operon* in the global
70 ocean, even under low ambient oceanic Hg(II) and MeHg concentrations, has been demonstrated for
71 *Alteromonadales* (*merA, merB*), *Rhodobacterales* (*merA*), *Flavobacteriales* (*merA*, *merB*), and
72 *Sphingobacteriales* (*merB*) among others [26,27].
73 The main objective of this study was to investigate potential Hg species reaction rates and drivers. We
74 selected two contrasted marine environments with different productivity and Hg species distribution,
75 I) offshore, oligotrophic waters of the northwestern Mediterranean Sea (MED) and II) coastal,
76 mesotrophic waters of the Bay of Biscay, northeastern Atlantic Ocean (ATL). We conducted sampling
77 campaigns during spring bloom in the MED in May 2021 and in the ATL in May 2022. We measured
78 ambient Hg species concentrations (THg, MMHg, DMHg, DGM) along vertical profiles, conducted
79 enriched isotope tracer incubation experiments and microbial diversity analysis (16S rDNA sequencing)
80 at biogeochemically relevant depths. We use the determined rate constants and reaction pathways in
81 a 1D water column model set-up to test the plausibility of our rates.

2. Material & Methods

2.1. Study Sites

Sampling was conducted on the 4th of May 2021 (MED station; 43° 0’ 16.128” N, 5° 25’ 21.792” E, 1500 m), northwestern Mediterranean Sea onboard the research vessel Antédon II, shortly after a wind driven upwelling event (1st to 3rd May) [28]. For the North Atlantic (ATL) station sampling was conducted on the 10th of May 2022 in the southeastern Bay of Biscay (ATL station; 43° 35’ 43.8” N, 1° 47’ 42.6012” W, 760 m) in onboard the research vessel Côte de la Manche. The MED station is an oligotrophic off-shore station , with no major riverine influence nearby [29], while the ATL station is a mesotrophic station under the influence of the Adour River [30]. A description of the two study areas is given in the SI.

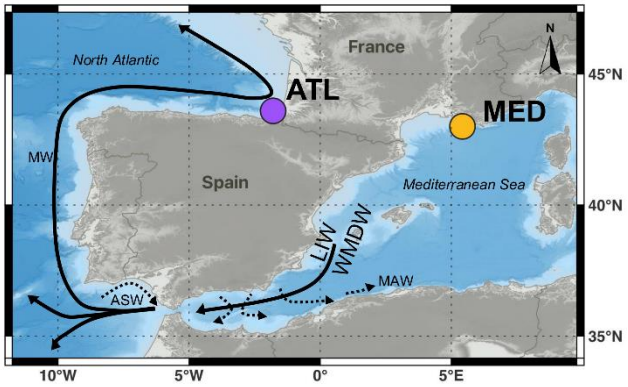

Figure 1. Illustrates the two sampling points in the two studied environments in the Mediterranean Sea and the North Atlantic. Arrows indicate main patterns of oceanic currents [31], dashed lines indicate surface currents and solid lines subsurface currents. LIW = Levantine Intermediate Waters, WMDW = Western Mediterranean Deep Waters, MW = Mediterranean Waters, MAW = Modified Atlantic Waters, ASW = Atlantic Surface Water. Map created with Qgis. Underlaying bathymetry from GEBCO.

2.2. Water Sampling and Sample Handling

Samples were obtained from acid cleaned (1 % HCl) 10 L GOFLO (General Oceanics) bottles mounted to an epoxy-painted trace metal clean carousel, following ultra-trace metal clean protocols [32]. Sampling bottles were thoroughly rinsed with the corresponding water without filtration and filled without head-space. Samples for total Hg (THg) (MED, ATL) were sampled into 60 mL FEP bottles (Nalgene) and kept at +4°C until analysis. For the ATL, DGM was sampled into 500 mL FEP/PFA bottles (Nalgene), purged onto gold coated sand traps (Au-traps) and stored at -20°C until analysis. For the MED, DGM was sampled into 125 mL PET bottles (VWR) and kept at +4°C until analysis. DMHg (MED, ATL) was sampled into 500 mL FEP/PFA bottles (Nalgene), directly purged onto graphitized carbon (Carbotraps) and kept at -20°C until analysis. The DMHg-purged sample was acidified to 0.5% (v/v) with HCl (OptimaTM) for MMHg analysis and an unpurged sample was acidified in the same way for MeHg analysis [33] and stored dark in double zip closed bags at +4°C until analysis.

For the ATL, seawater for incubation experiments was sampled at the surface (SML), Chlorophyll maximum (DCM), Oxygen minimum (min O_2), deep water (DW) (Figure 2) and filled into 1 L FEP/PFA bottles (Nalgene), or 5 L PE containers. Dedicated samples were filtered using an acid cleaned filtration tower (Nalgene) with acid cleaned 0.2 µm PP (Pall) or 0.22 µm PVDF membranes (Merck Millipore). The respective sampling bottles containing seawater for incubations were then stored in double zip closed bags, dark at +4°C until the start of the experiments the following day.

Filters to investigate the bacterial community composition (16S rDNA) were sampled in replicates by the filtration of 1 L of seawater onto a PP 0.2 µm membrane (MED; Pall) or sterile 0.2 µm cellulose acetate filter (ATL; Sartorius, Thermo Fisher Scientific) and stored in sterile cryotubes at -80°C until extraction.

2.1. Determination of Ambient Hg Species

Measurements were conducted following established protocols, all reagents were prepared with ultrapure water obtained from a Milli-Q system (Millipore, 18.2 MΩ cm) using analytical grade reagents. THg was analyzed following a modified USEPA method 1631 by Bromine monochloride (BrCl)

oxidation, stannous chloride ($SnCl_2$) reduction purge and trap followed by cold vapor atomic fluorescence spectrometry (CV-AFS, Brooks Rand, Model 3) the day after sampling [34]. For the MED, DGM samples were analyzed the day after sampling on the same instrument without oxidation and reduction and a higher sample volume (~125 mL), as previously described elsewhere [35]. For the ATL, DGM samples were analyzed by double amalgamation on gold-CV-AFS [36,37] within 10 days of sampling, DMHg was analyzed by cryogenic trapping GC-ICPMS [33,38] within 30 days of sampling. MeHg and MMHg were analyzed by species-specific isotope dilution analysis followed by GC-ICPMS [33,39] within 30 days of sampling.

2.2. Incubation Experiments

All incubations were conducted in triplicates, following an established protocol [40]. Briefly, samples were amended to ~10 pM of ^{199}Hg(II) and ~1 pM of MM^{201}Hg and incubated the day after sampling under natural light or dark conditions in water baths on the rooftop of MIO (MED; Mediterranean Institute of Oceanography, Marseille) or on the lower deck on board the research vessel (ATL). Additional experiments to follow the formation of DMHg were conducted for the MED under dark conditions for DCM, min O_2 and DW. For the ATL, the applied protocol allows to differentiate between the formation of Me^{199}Hg or MM^{199}Hg from added ^{199}Hg(II) [40]. All experiments were conducted on unfiltered and filtered waters (0.2 µm), the latter considered as abiotic control, removing the majority of particles and living cells [41–43]. Incubation samples (aqueous) were analyzed by GC-ICPMS applying quadruple species-specific isotope dilution [20,21], and traps (Au-, carbo-) were analyzed by cryogenic trapping GC-ICPMS [22].

Reaction rates were calculated assuming pseudo-first order reaction kinetics from a two-point (demethylation, methylation of Hg(II)) or a one point incubations (reduction, reductive demethylation, methylation of MMHg to DMHg). Demethylation was calculated as the slope of ln(MM^{201}Hg/MM^{201}Hg$_{t0}$), all other rates constants were calculated assuming a linear increase of the reaction product (reduction, reductive demethylation, methylation of Hg(II) and MMHg). Additional information on incubations can be found in the SI.

2.3. Ancillary Parameters

Temperature, Salinity, Oxygen and Fluorescence were measured *in situ* with a conductivity temperature density (CTD) probe (Seabird SBE 911plus), equipped with an Oxygen Sensor (Seabird SBE 43), beam transmissometer (SeaBird Scientific C-Star) and fluorometer (Chelsea Aquatracka III). DNA from *in situ* samples was extracted using the DNeasy PowerSoil Pro Kit (QIAGEN, Germany) according to the manufacturer's instructions and stored at -20°C. The 16S rDNA sequencing analysis through MiSEQ was performed following established methods and details can be found in the SI.

2.4. Quality assessment and Quality control

Method detection limit for ambient THg was 30 fM based on 3 x SD of the blank signal, for DGM 5.5 fM based on 3 x SD of purge blank measurements, for DMHg 0.38 fM based on the background equivalent concentration (BEC), and for MeHg and MMHg 15 and 12 fM based on the BEC. Relative standard deviation (RSD) for replicate samples for THg was usually better than 6 % at ~1 pM, and was determined for DGM with 9.6 % at 0.09 pM (n = 3), for DMHg with 7 % at 0.11 pM (n = 3), for MeHg with 4.7 % at 0.07 pM, and for MMHg with 7.9 % at 0.05 pM (n = 3). The RSD for each species was similar or better than the established measurements uncertainty for THg [44], DGM [45], MMHg and DMHg [33].

2.5. 1D Water column Model

We conducted a modeling exercise in order to test the feasibility of newly determined DMHg formation rates (~6 times faster than in current models) in this study and their impact on ambient Hg species distribution. To model the Hg speciation at the MED station, we use the GOTM-ECOSMO-MERCY modeling system. We chose to model only the MED station, as lateral and bottom influences can be considered to be of minor importance in contrast to the ATL station. GOTM is a hydrodynamic 1D model that calculates the turbulence of a vertical water-column by solving the 1D transport equation of momentum, salinity, and temperature. Thus, the model only has a vertical and no horizontal resolution [46,47].

ECOSMO is an end to end ecosystem model including the 7 biological functional groups for phytoplankton, zooplankton, macrobenthos, and fish [48]. MERCY is a Hg cycling model including speciation of Hg(0), Hg(II) HgS, MMHg(I), and DMHg in water, sediment, and biota, the partitioning of Hg(II) and MMHg(I) between the dissolved, particulate, and colloidal phases, and the air-sea exchange of Hg(0) and DMHg [49]. Based on our hypothesis that DMHg formation is biotically mediated, we scale our maximum DMHg formation rate determined to remineralization.

The coupled GOTM-ECOSMO-MERCY model was run for 20 years whereof the first 19 years were discarded as spin-up period. For a detailed description of the GOTM model, the modeled Hg species, and the reaction rates, please refer to the SI.

3. Results & Discussion

3.1. Biogeochemical Characteristics of the Two Study Sites

The MED station is representative for warm, oligotrophic waters, while the ATL station is representative for mesotrophic waters. We observed higher salinity (S) and temperatures (T) in the deepest sampled waters of the MED (800 m depth, S: 38.6, T: 13.4°C) compared to the ATL (750 m depth, S: 35.7, T: 10.3°C). The ATL station also showed a moderate freshwater influence (S: 34.7) from the Adour river extending down to ~79 m until reaching typical Atlantic salinity values (35.4). A relative fluorescence maximum, indicating the DCM depth was observed with typical $\delta^{13}C$ signatures of phytoplankton for the respective environment [50] at both stations, at ~53 m for the MED ($\delta^{13}C$: 23.44 to 24.7 ‰) and ~43 m for the ATL ($\delta^{13}C$: 24.65 ‰).

At the MED station, oxygen decreased (~149 µmol kg^{-1}) accompanied by a slight salinity increase to up to 38.7 down to ~475 m indicative of Eastern Levantine Intermediate Waters forming a relative min O_2 zone [51]. Below ~500 m oxygen concentrations increased until the deepest point of sampling (~800 m), representative of Western Mediterranean Deep Waters (Figure SI 2).

For the ATL, we observed a relative subsurface min O_2 at ~104 m (~191 µmol kg^{-1}) which coincided with a decrease in beam transmission. Below this relative min O_2, oxygen increased within the Eastern North Atlantic Central Water, followed by a decrease in oxygen and beam transmission down to the bottom. This decrease in oxygen could be due to the mixing with Mediterranean overflow waters below ~500 m (Figure SI 2), or the influence of remineralization of remobilized particles, described for the Capbreton Canyon [52,53].

3.2. Ambient Hg Species

Median THg concentrations were comparable between the two study stations, although more variable at the MED with 0.64 pM (interquartile range (IQR) = 0.50 - 0.94 pM) than at the ATL with 0.66 pM (IQR = 0.58 – 0.71 pM). The vertical profiles of THg differed between both stations (Figure 2). For the MED, THg was depleted at the surface, potentially due intense atmospheric exchange, and continuously increased with depth. At the ATL, THg peaked at the DCM depth (~1 pM) without showing a depletion at the surface due to the input of Hg from the Adour River plume [30]. Despite that a decrease in beam transmission below ~600 m possibly suggests a sediment influence, no clear impact on THg concentrations was observed at the deepest sampling point for the ATL station (Figure 2D). Our observations for the MED for THg are in the range of previous observations for the MED [12,29,51,54]. In contrast, our observations for the ATL for THg are lower than earlier observations reported at the same station during a higher discharge event of the Adour river [30] but align with previous observations for the North Atlantic, and the Iberian Abyssal Plain [29,55,56].

We observed an increase of MeHg with depth at both stations, while MMHg was uniformly distributed along the profiles and remained low (<0.06 pM), at the MED (median = 0.037 pM, IQR = 0.031 – 0.040 pM) and ATL station (median = 0.034 pM, IQR = 0.026 – 0.039 pM). In contrast, DMHg increased with depth, reaching concentrations at the MED roughly two times higher (0.45 ± 0.06 pM; maximum ± measurement uncertainty (k = 2)) than at the ATL station (0.16 ± 0.02 pM; maximum ± measurement uncertainty (k = 2)). DMHg always dominated the MeHg pool below ~200 m (Figure 2B, D; Figure SI 3), thus MeHg variations were primarily driven by DMHg levels. Our observations for MMHg concentration levels align with previous studies for the MED [29] and the eastern North Atlantic, which reported similarly low MMHg concentrations (generally below 0.1 pM) [29,55]. DMHg concentrations for both stations were higher [55,57] or within the range of literature values for the respective oceanic basin [29]. The importance of DMHg within the MeHg pool has previously been suggested for the MED [12,29,54,58], ATL [20,29] and other oceanic basins [20,59,60] although contrasting observations have also been reported [55,57,61].

239 Similarly, the importance of DMHg within the DGM pool has been debated, in particular for the MED
240 [51]. Our observations were in the range of literature values [29,30,57,62]. DGM concentrations were
241 comparable between the MED (median = 0.27 pM; 0.05 – 0.37 pM) and the ATL station (median = 0.21
242 pM; IQR = 0.16 – 0.27 pM), although DMHg was more prominent within the DGM pool for the MED
243 (median = 75 %, IQR = 43 – 120 %) than the ATL station (median = 8 %, IQR = 2 – 38 %), overall indicating
244 that Hg(0) was of higher importance in ATL mesotrophic waters than in MED oligotrophic waters.
245 Based on our results, we suggest that DMHg is an important Hg species in particular within the MeHg
246 pool and is key for explaining the differences in observed ambient MeHg maxima and its proportion of
247 THg. This is supported by the consistently low MMHg concentrations in both environments, in contrast
248 to the higher and more variable DMHg levels that dominated the MeHg pool at depth.

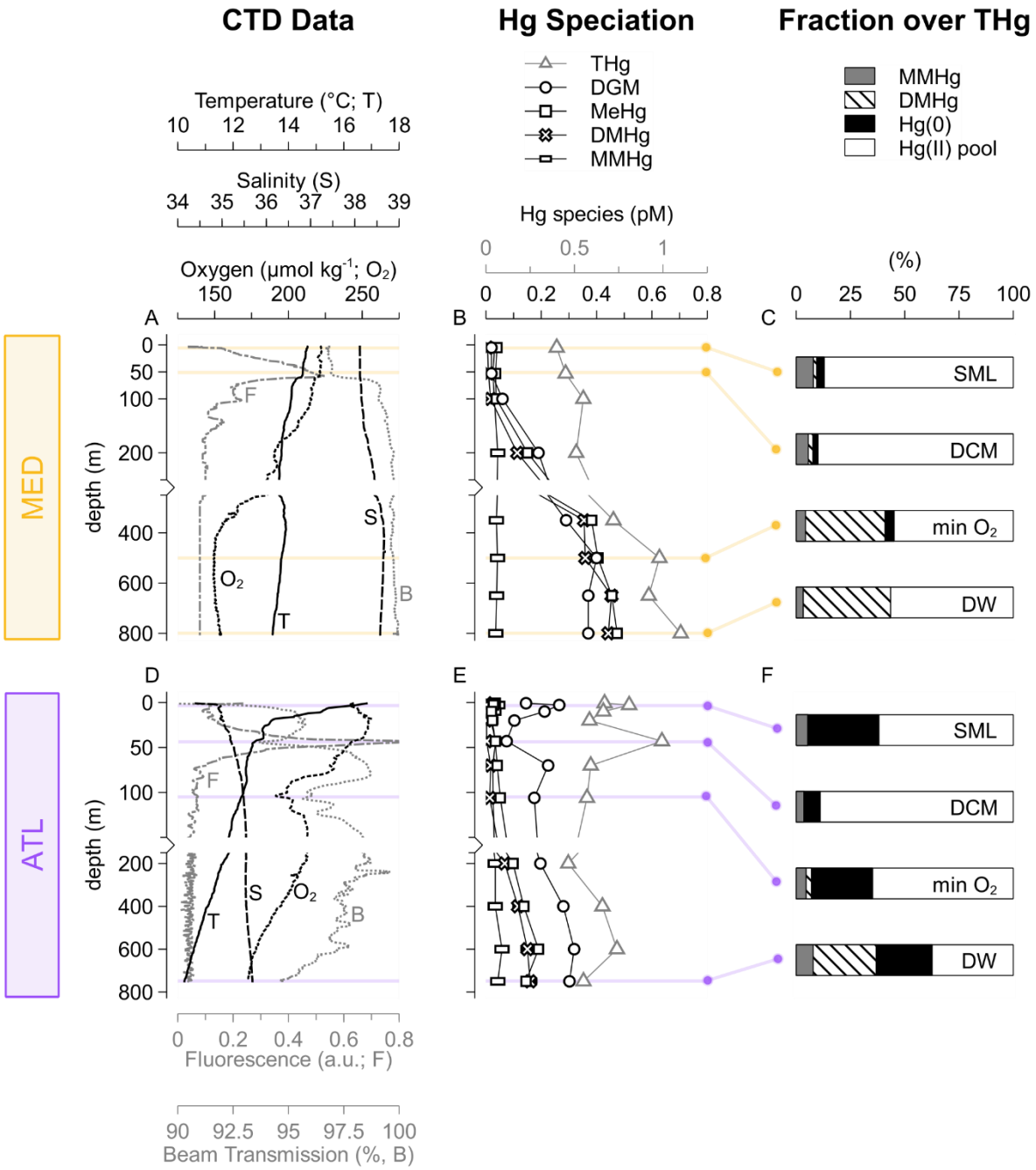

Figure 2. Illustrates CTD Data, Hg speciation and the relative fraction for each Hg species over the THg pool for the depths chosen for incubation experiments. The upper row corresponds to the MED and the lower row to the ATL study site. B, E) Primary x-axes (0 – 1.25) correspond to THg and secondary x-axes corresponds to DGM, MeHg, DMHg, and MMHg. Please note that the y-axes are broken at 250 m (MED) and 150 m (ATL) to emphasize surface variability. For Hg speciation profiles and relative fractions, including measurement uncertainties at k = 2, refer to Figure SI 3.

3.3. Hg Species Transformations

We detected methylation of Hg(II) to MeHg and DMHg, as well as the conversion of MMHg to DMHg, exclusively for unfiltered subsurface waters. We consider unfiltered water to be representative of *in situ* conditions, including the presence of particles and living cells. These findings, combined with the significance of bacterial activity in marine subsurface waters [63] suggest a particle-dependent, likely biotically driven *in situ* methylation pathway. This aligns with the prevailing scientific consensus that biotic *in situ* methylation predominantly governs MeHg in seawater [6,64].

We observed the highest potential methylation for the formation of DMHg from MMHg, at the MED station within min O_2 waters and DW (Figure 3A), followed by the formation of MeHg from Hg(II) in DW at the ATL station (Figure 3D). Highest potential methylation coincided with the highest relative abundance (>8 %) of potential *hgcAB* bearing phyla according to microbial community analysis (16S rDNA) at both stations (Figure 3A, D). Dedicated experiments to investigate the formation of DMHg from MMHg were conducted under dark conditions at the MED station (for DCM, min O_2 and DW). For experiments conducted at the ATL station we examined our purged incubation samples ($MM^{199}Hg$, n = 3) and compared them to unpurged samples ($Me^{199}Hg$, n = 3), used to calculate methylation rates from Hg(II) to MeHg. We found a significant difference (one tailed t-test, $p < 0.05$) between $Me^{199}Hg$ and $MM^{199}Hg$ in DW. In DW, $MM^{199}Hg$ accounted with ~10 % for the minor fraction of $Me^{199}Hg$ suggesting the dominant formation of DMHg from Hg(II). In contrast to the methylation observed for min O_2 waters at the ATL station, where the absence of a significant difference suggests that methylation to $MM^{199}Hg$ was predominant, although the importance of this pathway remains uncertain since methylation levels were close to the detection limit.

The potential *in situ* formation of DMHg (min O_2: MED; DW: MED, ATL) observed in incubation experiments aligns with the depths where DMHg dominated the ambient MeHg pool (Figure 2C, F). Our observed rate constants for the formation of MeHg (from Hg(II) and MMHg) are in agreement with literature data for MeHg formation from Hg(II) (see Table SI 6). In contrast, our highest observed rate

constants of DMHg formation from MMHg, were ~3 times higher (see Table SI 8), than highest, species-specific rate constants reported for polar marine waters [10].

Light-induced rates for Hg(II) reduction and MMHg demethylation were approximately one order of magnitude faster than dark rates, consistent with previous observations [10,11,30,65,66]. The reduction of Hg(II) was ubiquitous under natural light (Figure SI 5) and dark conditions(Figure 3C, F), with consistently higher rates in the unfiltered samples. Lower rates in filtered samples (0.2 µm) thus suggest a biotic contribution [67–71] whereas it remains unclear whether reduction was directly mediated by microbial pathways or indirectly induced by biotic activities, e.g. through biogenic organic compounds released by cells. In contrast, the light-dependent demethylation rates of MMHg were relatively similar for unfiltered and filtered incubations (Figure SI 5). Dark demethylation of MMHg was exclusively observed for unfiltered incubations, at similar rates at the DCM at both stations (Figure 3B, E) and in DW only at the ATL station (Figure 3E).

Microbial community analysis, conducted on incubated water samples confirmed the presence (>0.1 %, Figure 3) of *Rhodobacterales* (*merA*), *Flavobacteriales* (*merA, merB*) in all samples and *Sphingobacteriales* (*merB*) only in surface waters (0.3 ± 0.05 %, n = 3) at both stations. In agreement with the highest potential rate observed in incubation experiments for reduction and demethylation in surface waters (SML, DCM), and lowest potential rate in deepest samples (DW). The highest relative abundance of *Rhodobacterales* (*merA*) in the SML at ATL station (11.2 ± 0.2 %, n = 3) coincided with the highest dark reduction rate observed in this study. *Mer*-independent reduction pathways, such as the production of reactive oxygen species by heterotrophic bacteria [72,73], extracellular reduction through superoxide formation [74], the use of Hg(II) as an electron acceptor by phototrophs [75,76], and light-dependent processes previously linked to primary productivity [67,71,77], may also be of relevance under our experimental conditions. Similarly, *mer*-independent demethylation pathways may include intracellular *mer*- (see SI 6) and light-independent demethylation mediated by phytoplankton, as demonstrated in laboratory experiments [78], and demethylation by sulfate

306 reducing organisms [79], particularly in DW at the ATL station where we observed dark biotic
307 demethylation.

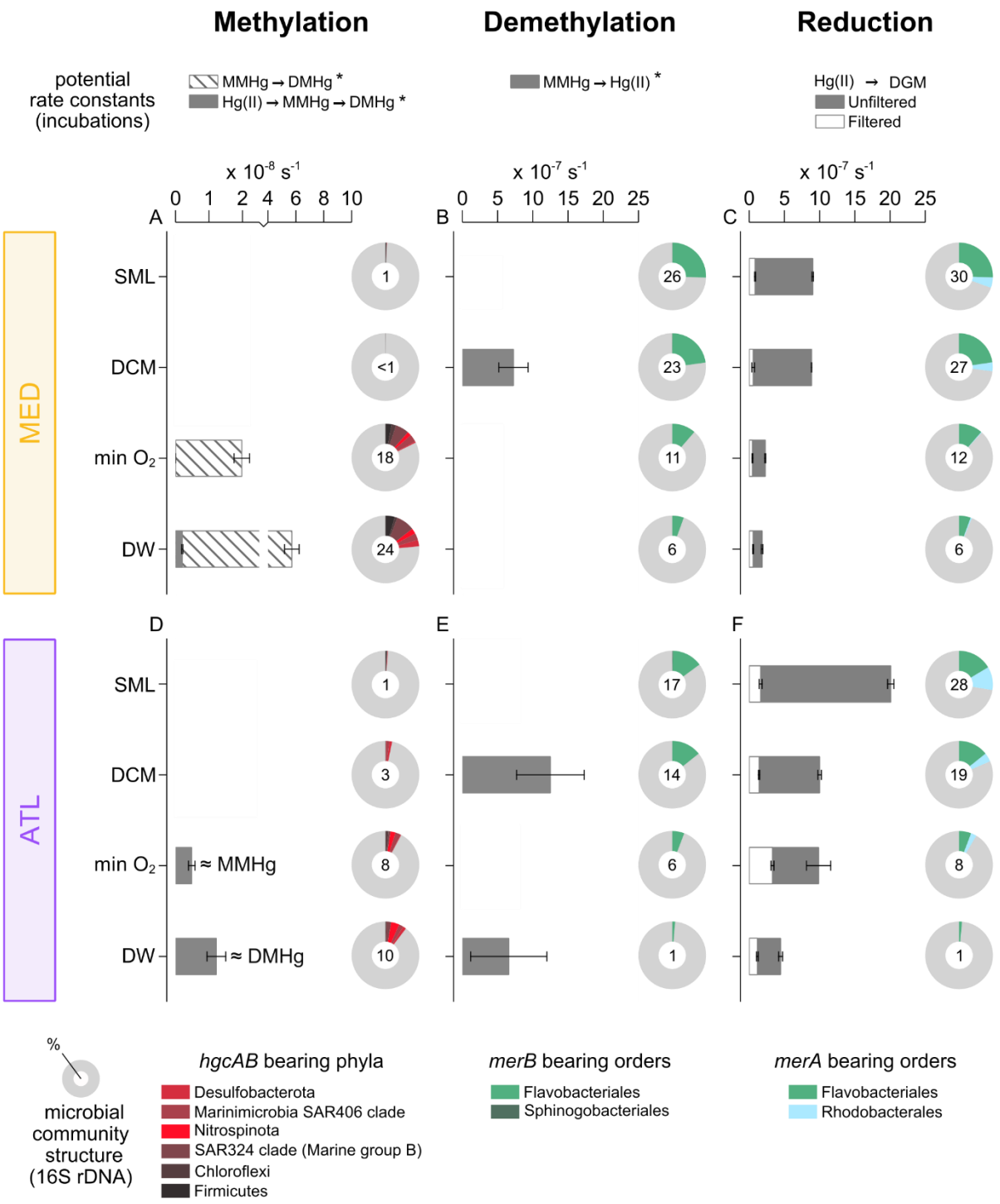

Figure 3. Illustrates potential transformation rates as determined in incubation experiments and the potential to mediate Hg species transformations within the microbial community based on 16S rDNA analysis. Upper row corresponds to the studied site in the Mediterranean (MED) and lower row to the Atlantic (ATL). Please note the different x-axes and broken x-axes for A and D. The potential for methylation within the microbial community is presented at phyla level for known *hgcAB* bearing microorganisms [15–17,80,81], and for reduction and demethylation was based on orders previously shown to be actively expressing the *mer*- operon under environmentally relevant conditions [27]. *Potential transformation as evidenced by incubation experiments only observed in the presence of particles. If no symbol is shown for a certain depth, it indicates that the reaction was not detected at that specific depth.

3.4. The Need to Separate MMHg and DMHg Dynamics

The origin of marine MeHg is still debated [82] and the underlying mechanisms governing ambient MMHg and DMHg levels in marine oxygenated waters are not well understood. Methylation of Hg(II) to MMHg, mediated by *hgcAB* bearing microorganisms, is known to occur under anaerobic conditions [15,79,83]. Anoxic micro-niches within sinking particles, have been proposed as potential sites for Hg (II) methylation [14,17] in marine oxygenated waters [84].

At the MED site, we observed the formation of DMHg from MMHg in both the min O_2 and DW waters. However, simultaneous methylation of Hg(II) to DMHg was only detected in DW, and was the slowest methylation rate observed and below the DL for MeHg formed in aqueous samples (DL lower by approximately one order of magnitude). Our observations at the MED site and the limited available literature suggest a two-step mechanisms (Hg(II)→ MMHg→ DMHg) for the formation [10,19] as well as the degradation of DMHg [21,22,60,85,86]. While our results indicate the crucial role of particles for both methylation steps, different biotic or abiotic drivers (e.g. particle size distribution, organic substrate, bacterial diversity and heterotrophic activity) may influence each individual step. It is also possible that the two methylation steps may occur spatially or temporally independent of each other or display distinct sensitivity/reactivity to/with oxygen [10,11,19]. In addition, methylation of Hg(II) may also have occurred in deeper waters but at rates below our DL. We find that studying the dynamics of MMHg and DMHg separately is essential for explaining MeHg maxima in marine oxygenated waters. The importance of distinguishing MMHg and DMHg dynamics, is furthermore exemplified by the discrepancy between MMHg demethylation and MeHg formation rates observed for DW at the ATL station. In our experiments, MMHg demethylation rates were ~2 times higher than the formation of MeHg from Hg(II), suggesting a net demethylation of MeHg. However, MeHg mainly present as DMHg comprised ~26 % of ambient THg in DW, together with the preferential formation of DMHg from Hg(II) in our experiments, point towards the crucial role of DMHg in the system. Published dark demethylation rates (MMHg → Hg(II)) are ~23 times higher (median values, log-transformed) than dark methylation rates (Hg(II) → MeHg) (Table SI 6 and SI 7). Literature data thus indicate a net

demethylation globally, which contrasts with the widespread presence of MeHg in the ocean [7]. Overall our observations and literature data suggest that a net methylation rate, based solely on the MeHg formation (Hg(II) → MeHg (MMHg + DMHg)) and demethylation of MMHg (MMHg → Hg(II)), does not fully resolve the biogeochemical MeHg cycle [20,21,59,87,88].

3.5. Water Column Model

Observations of *in situ* DMHg formation rates in oxygenated marine waters are scarce (Table SI 8), with our observed maximum rates (MMHg → DMHg) being ~6 times higher than rates applied in current biogeochemical models [8,9]. The important formation of DMHg raises questions about the stability of DMHg influencing its fate in seawater. Unlike particle-reactive MMHg (and Hg(II)), which can be scavenged and exported to deeper waters and sediments, DMHg, as a neutral dissolved gas, and may persist in the water column [89]. Early studies suggested that DMHg is highly stable in the deep ocean [20], while the photolytic degradation of DMHg [21,60], demethylation in surface waters [87], and evasion to the atmosphere [86,90] are important loss mechanisms. There is a lack of experimentally determined *in situ* rates but stability experiments indicated that DMHg remained stable over a period of at least 20 days [91] to weeks [22].

Our experimental set-up was not designed to assess the stability of DMHg. Based on the importance of DMHg within the ambient MeHg pool, we hypothesize that both the formation and stability of DMHg are key to explain MeHg maxima. To test this hypothesis and the plausibility of our rates, we modeled ambient Hg species along a vertical profile for the MED station.

We included two DMHg demethylation rates in our model runs, previously applied in coupled biogeochemical models [8,9,49] a low rate of 2.2 x 10^{-9} s^{-1} (high DMHg stability) and a high rate of 1.9 x 10^{-8} s^{-1} (low DMHg stability) while keeping our fastest observed DMHg formation rate (5.71 x 10^{-8} s^{-1} at +20°C). Reduction, oxidation, methylation of Hg(II) to MMHg and demethylation of MMHg were kept constant for both model scenarios (Table SI 5).

Overall the agreement between modeled THg and observational data was good, within a factor of 2 (see Figure SI 9), with better agreement in deep waters (>101 m) than for surface waters (0 – 101 m), where THg was overestimated by ~110 % (Figure 4). Modeled Hg(0) deviated from observations, with a good fit in the surface compared to our (Figure SI 10) and previous observations at the same station (Figure SI 11, Figure SI 12) [29].

For MeHg species, subsurface observations for this and a previous study, could only be reproduced under the high DMHg stability scenario (Figure 4A, Figure SI 11). The slight underestimation of MMHg (<30 %, average) may be attributed to an underestimation of MMHg formation rates or its stability.

The 1D water column model supports the plausibility of our high DMHg formation rates, and indicates that DMHg must be very stable. High DMHg stability mediates high DMHg concentrations, even if methylation of Hg(II) to MMHg is slower than the demethylation of MMHg to Hg(II).

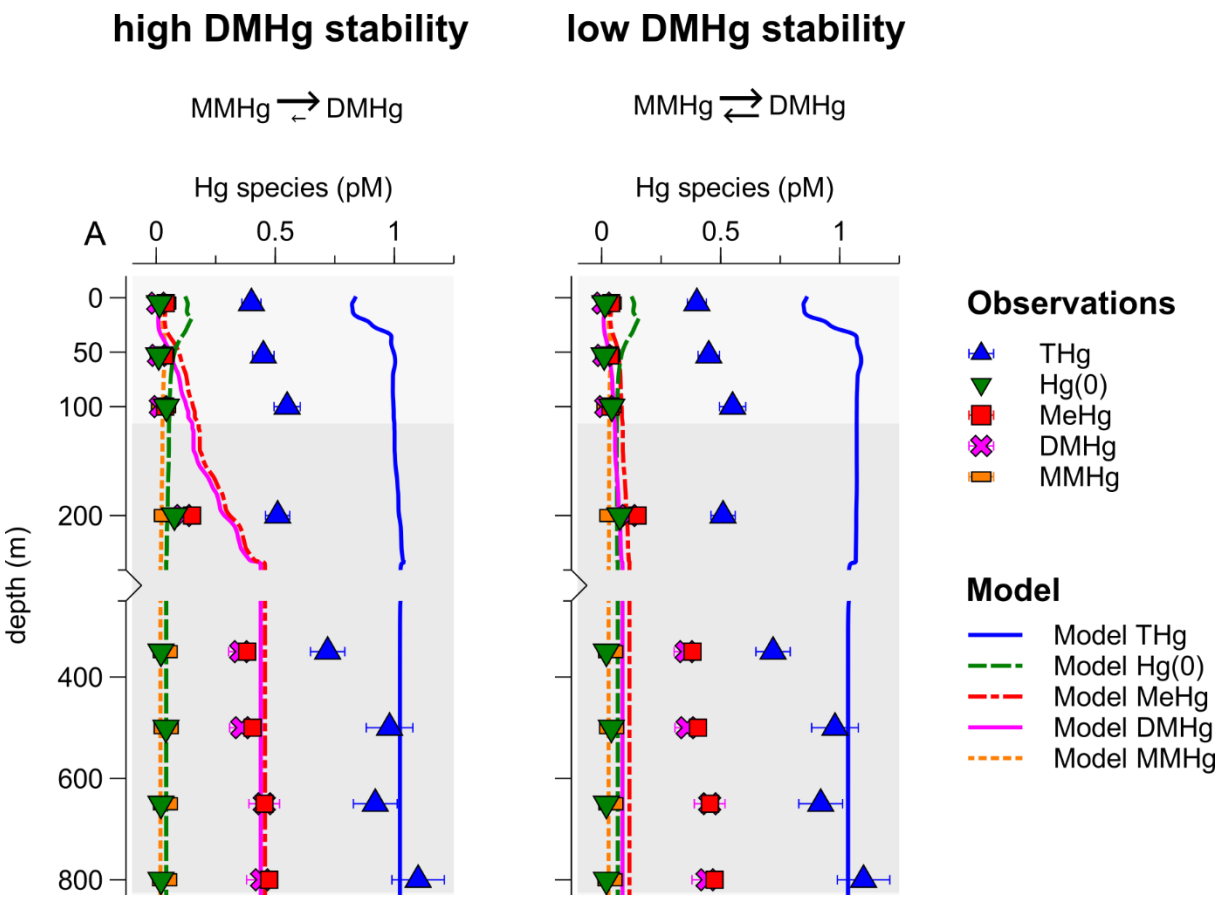

381 Figure 4. Illustrates model output for Hg species and observations (error bars represent
382 measurement uncertainties at k = 2) for the MED station. The results are presented in pM for the A)
383 high DMHg stability and B) low DMHg stability.

3.6. Environmental Implications

Our study highlights the important role of DMHg in the marine biogeochemical cycle of MeHg. We demonstrate the potential for formation of DMHg in deep waters of two distinct environments, consistent with the dominance of DMHg within the MeHg pool. Under our experimental conditions, the formation of both MMHg and DMHg was limited to the subsurface waters and appeared to be biotically mediated, as it was exclusively detected in the presence of particles and living cells.

Our modeling exercise suggests that both, the formation of MMHg and DMHg, as well as their stability, are key to explain ambient MeHg concentrations. Our study indicates that DMHg formation rates applied in current coupled biogeochemical models may be underestimated. In addition, current models may underestimate the stability of DMHg [8,9]. Both methylation (of Hg(II) and MMHg) and demethylation rates (of MMHg and DMHg) were kept constant in our model, and reproduced MeHg observations well. However, it is likely that these rates exhibit a seasonal variability [11] driving ambient seasonal MeHg variations in the MED [13] and elsewhere [88,92]. Future work should include more MMHg and DMHg observations and further investigate seasonal changes, along with MMHg and DMHg formation rates. We anticipate that systematically integrating microbial diversity and activity data, with Hg species transformation rates, will help to better understand the marine Hg cycling which is needed to update current models guiding future Hg mitigation strategies in the frame of the Minamata Convention on Mercury.

Acknowledgement

We thank Deny Malengros (MIO CNRS-AMU), Jingjing Yuan (MIO CNRS-AMU), Isabel Garcia Arevalo (IFREMER), Rosanna Margalef-Marti (IPREM CNRS-UPPA), Aubin Thibault de Chanvalon (IPREM CNRS-UPPA), and the captain and the crew of the R/V "Côtes de la Manche" and R/V "Antédon II" (Flotte Océanographique Française) for logistical, sampling and technical supports. We are grateful to Pierre Anschutz and Nathalie Labourdette (EPOC University of Bordeaux) for DOC measurement and to Javier Tesán-Onrubia and Daniela Bănaru for providing particulate carbon and nitrogen data for the Mediterranean station. The authors are grateful to Paco Bustamante, Philippe Pineau, Benoit Lebreton and Gaël Guillou from the laboratory LIENSs (Littoral Environnement et Sociétés, La Rochelle) for their support with stable isotope analyses.

This work was performed in the framework of the GMOS-Train ITN project and has received funding from the European Union's Horizon 2020 research and innovation program under the Marie Sklodowska-Curie grant agreement no. 860497. Lars-Eric Heimbürger-Boavida acknowledges funding via the French National Funding Agency project HydrOThermal Mercury (ANR-21-CE34-0026). Javier Tesán-Onrubia and Daniela Bănaru acknowledge funding for the CONTAMPUMP project (ANR JCJC #19-CE34-0001-01). This work is also a contribution to the Energy Environment Solutions (E2S-UPPA) initiative of excellence (I-SITES, PIA France) for the Scientific Hub "Metals in Environmental Systems Microbiology (MESMic)".

CRediT statement

Alina Kleindienst: Conceptualization, Methodology, Investigation, Validation, Writing – Original Draft, Writing – Review & Editing

Emmanuel Tessier: Investigation, Resources, Validation, Writing – Review & Editing

Océane Asensio: Investigation

Natalia Torres - Rodriguez: Investigation, Writing – Review & Editing

Aurélie Dufour: Investigation

Lars-Eric Heimbürger-Boavida: Conceptualization, Methodology, Resources, Writing – Review & Editing, Funding acquisition

Johannes Bieser: Methodology, Investigation, Writing – Review & Editing

Claire Gassie: Validation, Investigation, Resources

Remy Guyoneaud: Conceptualization, Resources, Writing – Review & Editing, Funding acquisition

David Amouroux: Conceptualization, Resources, Methodology, Writing – Review & Editing, Project administration, Funding acquisition

Supporting Information

Additional details on the study sites, experimental setup, and model configuration, as well as a summary of literature-reported rates for methylation and demethylation, are provided in the supporting information. The supporting information also includes results from microbial community analyses (16S rDNA), reductive demethylation experiments, and tables summarizing reaction rates and modeling data.

4. References

[1] J.A. Tesán-Onrubia, L.-E. Heimbürger-Boavida, A. Dufour, M. Harmelin-Vivien, I. García-Arévalo, J. Knoery, B. Thomas, F. Carlotti, M. Tedetti, D. Bănaru, Bioconcentration, bioaccumulation and biomagnification of mercury in plankton of the Mediterranean Sea, Marine Pollution Bulletin 194 (2023) 115439. https://doi.org/10.1016/j.marpolbul.2023.115439.

[2] R.A. Lavoie, A. Bouffard, R. Maranger, M. Amyot, Mercury transport and human exposure from global marine fisheries, Sci Rep 8 (2018) 6705. https://doi.org/10.1038/s41598-018-24938-3.

[3] AMAP/UN Environment, Technical Background Report to the Global Mercury Assessment 2018. Artic Monitoring and Assessment Programme, Oslo, Norway/ UN Environment Programme, Chemicals and Health Branch, Geneva, Switzerland., (2019). https://www.mercuryconvention.org/en/resources/technical-background-report-global-mercury-assessment-2018 (accessed October 10, 2022).

[4] C.H. Lamborg, C.R. Hammerschmidt, K.L. Bowman, G.J. Swarr, K.M. Munson, D.C. Ohnemus, P.J. Lam, L.-E. Heimbürger, M.J.A. Rijkenberg, M.A. Saito, A global ocean inventory of anthropogenic mercury based on water column measurements, Nature 512 (2014) 65–68. https://doi.org/10.1038/nature13563.

[5] W.F. Fitzgerald, R.P. Mason, The Global Mercury Cycle: Oceanic and Anthropogenic Aspects, in: W. Baeyens, R. Ebinghaus, O. Vasiliev (Eds.), Global and Regional Mercury Cycles: Sources, Fluxes and Mass Balances, Springer Netherlands, Dordrecht, 1996: pp. 85–108. https://doi.org/10.1007/978-94-009-1780-4_3.

[6] W.F. Fitzgerald, C.H. Lamborg, C.R. Hammerschmidt, Marine Biogeochemical Cycling of Mercury, Chem. Rev. 107 (2007) 641–662. https://doi.org/10.1021/cr050353m.

[7] K.L. Bowman, C.H. Lamborg, A.M. Agather, A global perspective on mercury cycling in the ocean, Science of The Total Environment 710 (2020) 136166. https://doi.org/10.1016/j.scitotenv.2019.136166.

[8] G. Rosati, D. Canu, P. Lazzari, C. Solidoro, Assessing the spatial and temporal variability of methylmercury biogeochemistry and bioaccumulation in the Mediterranean Sea with a coupled 3D model, Biogeosciences 19 (2022) 3663–3682. https://doi.org/10.5194/bg-19-3663-2022.

[9] Y. Zhang, A.L. Soerensen, A.T. Schartup, E.M. Sunderland, A Global Model for Methylmercury Formation and Uptake at the Base of Marine Food Webs, Global Biogeochemical Cycles 34 (2020) e2019GB006348. https://doi.org/10.1029/2019GB006348.

[10] I. Lehnherr, V.L.S. Louis, H. Hintelmann, J.L. Kirk, Methylation of inorganic mercury in polar marine waters, Nature Geoscience 4 (2011) 298–302. https://doi.org/10.1038/ngeo1134.

[11] M. Monperrus, E. Tessier, D. Amouroux, A. Leynaert, P. Huonnic, O.F.X. Donard, Mercury methylation, demethylation and reduction rates in coastal and marine surface waters of the Mediterranean Sea, Marine Chemistry 107 (2007) 49–63. https://doi.org/10.1016/j.marchem.2007.01.018.

[12] D. Cossa, B. Averty, N. Pirrone, The origin of methylmercury in open Mediterranean waters, Limnology and Oceanography 54 (2009) 837–844. https://doi.org/10.4319/lo.2009.54.3.0837.

[13] L.-E. Heimbürger, D. Cossa, J.-C. Marty, C. Migon, B. Averty, A. Dufour, J. Ras, Methyl mercury distributions in relation to the presence of nano- and picophytoplankton in an oceanic water column (Ligurian Sea, North-western Mediterranean), Geochimica et Cosmochimica Acta 74 (2010) 5549–5559. https://doi.org/10.1016/j.gca.2010.06.036.

[14] E.M. Sunderland, D.P. Krabbenhoft, J.W. Moreau, S.A. Strode, W.M. Landing, Mercury sources, distribution, and bioavailability in the North Pacific Ocean: Insights from data and models, Global Biogeochemical Cycles 23 (2009). https://doi.org/10.1029/2008GB003425.

[15] J.M. Parks, A. Johs, M. Podar, R. Bridou, R.A. Hurt, S.D. Smith, S.J. Tomanicek, Y. Qian, S.D. Brown, C.C. Brandt, A.V. Palumbo, J.C. Smith, J.D. Wall, D.A. Elias, L. Liang, The Genetic Basis for Bacterial Mercury Methylation, Science 339 (2013) 1332–1335. https://doi.org/10.1126/science.1230667.

[16] C.M. Gionfriddo, M.T. Tate, R.R. Wick, M.B. Schultz, A. Zemla, M.P. Thelen, R. Schofield, D.P. Krabbenhoft, K.E. Holt, J.W. Moreau, Microbial mercury methylation in Antarctic sea ice, Nat Microbiol 1 (2016) 1–12. https://doi.org/10.1038/nmicrobiol.2016.127.

[17] E. Villar, L. Cabrol, L.-E. Heimbürger-Boavida, Widespread microbial mercury methylation genes in the global ocean, Environmental Microbiology Reports 12 (2020) 277–287. https://doi.org/10.1111/1758-2229.12829.

[18] M.C. Despins, R.P. Mason, A.M. Aguilar-Islas, C.H. Lamborg, C.R. Hammerschmidt, S.E. Newell, Linked mercury methylation and nitrification across oxic subpolar regions, Frontiers in Environmental Chemistry 4 (2023). https://www.frontiersin.org/articles/10.3389/fenvc.2023.1109537 (accessed September 5, 2023).

[19] S. Jonsson, N.M. Mazrui, R.P. Mason, Dimethylmercury Formation Mediated by Inorganic and Organic Reduced Sulfur Surfaces, Sci Rep 6 (2016) 27958. https://doi.org/10.1038/srep27958.

[20] R.P. Mason, K.R. Rolfhus, W.F. Fitzgerald, Methylated and elemental mercury cycling in surface and deep ocean waters of the North Atlantic, Water Air Soil Pollut 80 (1995) 665–677. https://doi.org/10.1007/BF01189719.

[21] J. West, S. Gindorf, S. Jonsson, Photochemical Degradation of Dimethylmercury in Natural Waters, Environ. Sci. Technol. 56 (2022) 5920–5928. https://doi.org/10.1021/acs.est.1c08443.

[22] F.J. Black, C.H. Conaway, A.R. Flegal, Stability of Dimethyl Mercury in Seawater and Its Conversion to Monomethyl Mercury, Environ. Sci. Technol. 43 (2009) 4056–4062. https://doi.org/10.1021/es9001218.

[23] T. Barkay, B. Gu, Demethylation–The Other Side of the Mercury Methylation Coin: A Critical Review, ACS Environ. Au 2 (2022) 77–97. https://doi.org/10.1021/acsenvironau.1c00022.

[24] T. Barkay, I. Wagner-Döbler, Microbial transformations of mercury: potentials, challenges, and achievements in controlling mercury toxicity in the environment, Adv Appl Microbiol 57 (2005) 1–52. https://doi.org/10.1016/S0065-2164(05)57001-1.

[25] C.A. Christakis, T. Barkay, E.S. Boyd, Expanded Diversity and Phylogeny of mer Genes Broadens Mercury Resistance Paradigms and Reveals an Origin for MerA Among Thermophilic Archaea, Frontiers in Microbiology 12 (2021). https://www.frontiersin.org/articles/10.3389/fmicb.2021.682605 (accessed October 13, 2022).

[26] I. Sanz-Sáez, C. Pereira-García, A.G. Bravo, L. Trujillo, M. Pla i Ferriol, M. Capilla, P. Sánchez, R.C. Rodríguez Martín-Doimeadios, S.G. Acinas, O. Sánchez, Prevalence of Heterotrophic Methylmercury Detoxifying Bacteria across Oceanic Regions, Environ Sci Technol 56 (2022) 3452–3461. https://doi.org/10.1021/acs.est.1c05635.

[27] I. Sanz-Sáez, A.G. Bravo, M. Ferri, J.-M. Carreras, O. Sánchez, M. Sebastian, C. Ruiz-González, E. Capo, C.M. Duarte, J.M. Gasol, P. Sánchez, S.G. Acinas, Microorganisms Involved in Methylmercury Demethylation and Mercury Reduction are Widely Distributed and Active in the Bathypelagic Deep Ocean Waters, Environ. Sci. Technol. 58 (2024) 13795–13807. https://doi.org/10.1021/acs.est.4c00663.

[28] R. Fuchs, M. Thyssen, V. Creach, M. Dugenne, L. Izard, M. Latimier, A. Louchart, P. Marrec, M. Rijkeboer, G. Grégori, D. Pommeret, Automatic recognition of flow cytometric phytoplankton functional groups using convolutional neural networks, Limnology and Oceanography, Methods 20 (2022) 2022. https://doi.org/10.1002/lom3.10493.

[29] M. Jiskra, L.-E. Heimbürger-Boavida, M.-M. Desgranges, M.V. Petrova, A. Dufour, B. Ferreira-Araujo, J. Masbou, J. Chmeleff, M. Thyssen, D. Point, J.E. Sonke, Mercury stable isotopes constrain atmospheric sources to the ocean, Nature 597 (2021) 678–682. https://doi.org/10.1038/s41586-021-03859-8.

[30] A. Sharif, M. Monperrus, E. Tessier, S. Bouchet, H. Pinaly, P. Rodriguez-Gonzalez, P. Maron, D. Amouroux, Fate of mercury species in the coastal plume of the Adour River estuary (Bay of Biscay, SW France), Science of The Total Environment 496 (2014) 701–713. https://doi.org/10.1016/j.scitotenv.2014.06.116.

[31] D. Cossa, J. Knoery, M. Boye, N. Marusczak, B. Thomas, P. Courau, F. Sprovieri, Oceanic mercury concentrations on both sides of the Strait of Gibraltar decreased between 1989 and 2012, Anthropocene 29 (2020) 100230. https://doi.org/10.1016/j.ancene.2019.100230.

[32] G. Cutter, K. Casciotti, P. Croot, W. Geibert, L.-E. Heimbürger, M. Lohan, H. Planquette, T. van de Flierdt, Sampling and Sample-handling Protocols for GEOTRACES Cruises, (2017).

[33] A. Kleindienst, I. Živković, E. Tessier, A. Koenig, L.-E. Heimbürger-Boavida, M. Horvat, D. Amouroux, Assessing comparability and uncertainty of analytical methods for methylated mercury species in seawater, Analytica Chimica Acta 1278 (2023) 341735. https://doi.org/10.1016/j.aca.2023.341735.

[34] L.-E. Heimbürger, J.E. Sonke, D. Cossa, D. Point, C. Lagane, L. Laffont, B.T. Galfond, M. Nicolaus, B. Rabe, M.R. van der Loeff, Shallow methylmercury production in the marginal sea ice zone of the central Arctic Ocean, Sci Rep 5 (2015) 10318. https://doi.org/10.1038/srep10318.

[35] M.V. Petrova, S. Krisch, P. Lodeiro, O. Valk, A. Dufour, M.J.A. Rijkenberg, E.P. Achterberg, B. Rabe, M. Rutgers van der Loeff, B. Hamelin, J.E. Sonke, C. Garnier, L.-E. Heimbürger-Boavida, Mercury species export from the Arctic to the Atlantic Ocean, Marine Chemistry 225 (2020) 103855. https://doi.org/10.1016/j.marchem.2020.103855.

[36] S. Bouchet, E. Tessier, M. Monperrus, R. Bridou, J. Clavier, G. Thouzeau, D. Amouroux, Measurements of gaseous mercury exchanges at the sediment-water, water-atmosphere and sediment-atmosphere interfaces of a tidal environment (Arcachon Bay, France), J Environ Monit 13 (2011) 1351–1359. https://doi.org/10.1039/c0em00358a.

[37] B. Duval, E. Tessier, L. Kortazar, L.A. Fernandez, A. de Diego, D. Amouroux, Dynamics, distribution, and transformations of mercury species from pyrenean high-altitude lakes, Environ Res 216 (2023) 114611. https://doi.org/10.1016/j.envres.2022.114611.

[38] D. Amouroux, E. Tessier, C. Pécheyran, O.F.X. Donard, Sampling and probing volatile metal(loid) species in natural waters by in-situ purge and cryogenic trapping followed by gas chromatography and inductively coupled plasma mass spectrometry (P-CT-GC-ICP/MS), Analytica Chimica Acta 377 (1998) 241–254. https://doi.org/10.1016/S0003-2670(98)00425-5.

[39] M. Monperrus, P. Rodríguez-González, D. Amouroux, J. Garcia Alonso, O. Donard, Evaluating the potential and limitations of double-spiking species-specific isotope dilution analysis for the accurate quantification of mercury species in different environmental matrices, Analytical and Bioanalytical Chemistry 390 (2008) 655–66. https://doi.org/10.1007/s00216-007-1598-z.

[40] A. Kleindienst, E. Tessier, B. Duval, A. Koenig, R. Guyoneaud, D. Amouroux, Assessment of Incubation Experiments Using Isotopically Enriched Mercury Compounds in Seawater including

574 Dissolved Gaseous Mercury, ACS EST Water (2024).
575 https://doi.org/10.1021/acsestwater.4c00505.

576 [41] M. Hahn, Broad diversity of viable bacteria in 'sterile' (0.2 µm) filtered water, Research in
577 Microbiology 155 (2004) 688–91. https://doi.org/10.1016/j.resmic.2004.05.003.

578 [42] J. Liu, B. Li, Y. Wang, G. Zhang, X. Jiang, X. Li, Passage and community changes of filterable bacteria
579 during microfiltration of a surface water supply, Environ Int 131 (2019) 104998.
580 https://doi.org/10.1016/j.envint.2019.104998.

581 [43] Y. Wang, F. Hammes, M. Düggelin, T. Egli, Influence of Size, Shape, and Flexibility on Bacterial
582 Passage through Micropore Membrane Filters, Environ. Sci. Technol. 42 (2008) 6749–6754.
583 https://doi.org/10.1021/es800720n.

584 [44] N. Torres-Rodriguez, J. Yuan, S. Petersen, A. Dufour, D. González-Santana, V. Chavagnac, H.
585 Planquette, M. Horvat, D. Amouroux, C. Cathalot, E. Pelleter, R. Sun, J.E. Sonke, G.W. Luther, L.-
586 E. Heimbürger-Boavida, Mercury fluxes from hydrothermal venting at mid-ocean ridges
587 constrained by measurements, Nat. Geosci. (2023) 1–7. https://doi.org/10.1038/s41561-023-
588 01341-w.

589 [45] A. Kleindienst, Les composés méthylés du mercure dans les écosystèmes côtiers : approches
590 expérimentales de spéciation et transformations biogéochimiques, These de doctorat, Pau, 2024.
591 https://theses.fr/2024PAUU3003 (accessed October 22, 2024).

592 [46] H. Burchard, K. Bolding, M. Ruiz-Villarreal, GOTM, a general ocean turbulence model. Theory,
593 implementation and test cases, 1999.

594 [47] L. Umlauf, H. Burchard, B. K., GOTM: Source Code and Test Case Documentation, Version 4.0,
595 (2024). https://gotm.net/manual/stable/pdf/letter.pdf (accessed November 18, 2024).

596 [48] U. Daewel, C. Schrum, Simulating long-term dynamics of the coupled North Sea and Baltic Sea
597 ecosystem with ECOSMO II: Model description and validation, Journal of Marine Systems 119–
598 120 (2013) 30–49. https://doi.org/10.1016/j.jmarsys.2013.03.008.

599 [49] J. Bieser, D.J. Amptmeijer, U. Daewel, J. Kuss, A.L. Soerensen, C. Schrum, The 3D biogeochemical
600 marine mercury cycling model MERCY v2.0 – linking atmospheric Hg to methylmercury in fish,
601 Geoscientific Model Development 16 (2023) 2649–2688. https://doi.org/10.5194/gmd-16-2649-
602 2023.

603 [50] C. Liénart, N. Savoye, V. David, P. Ramond, P. Rodriguez Tress, V. Hanquiez, V. Marieu, F. Aubert,
604 S. Aubin, S. Bichon, C. Boinet, L. Bourasseau, Y. Bozec, M. Bréret, E. Breton, J. Caparros, T. Cariou,
605 P. Claquin, P. Conan, A.-M. Corre, L. Costes, M. Crouvoisier, Y. Del Amo, H. Derriennic, F.
606 Dindinaud, R. Duran, M. Durozier, J. Devesa, S. Ferreira, E. Feunteun, N. Garcia, S. Geslin, E.
607 Grossteffan, A. Gueux, J. Guillaudeau, G. Guillou, O. Jolly, N. Lachaussée, M. Lafont, V. Lagadec,
608 J. Lamoureux, B. Lauga, B. Lebreton, E. Lecuyer, J.-P. Lehodey, C. Leroux, S. L'Helguen, E. Macé,
609 E. Maria, L. Mousseau, A. Nowaczyk, P. Pineau, F. Petit, M. Pujo-Pay, P. Raimbault, P. Rimmelin-
610 Maury, V. Rouaud, P.-G. Sauriau, E. Sultan, N. Susperregui, Dynamics of particulate organic
611 matter composition in coastal systems: Forcing of spatio-temporal variability at multi-systems
612 scale, Progress in Oceanography 162 (2018) 271–289.
613 https://doi.org/10.1016/j.pocean.2018.02.026.

614 [51] D. Cossa, J. Knoery, D. Bănaru, M. Harmelin-Vivien, J.E. Sonke, I.M. Hedgecock, A.G. Bravo, G.
615 Rosati, D. Canu, M. Horvat, F. Sprovieri, N. Pirrone, L.-E. Heimbürger-Boavida, Mediterranean
616 Mercury Assessment 2022: An Updated Budget, Health Consequences, and Research
617 Perspectives, Environmental Science & Technology (2022).
618 https://doi.org/10.1021/acs.est.1c03044.

[52] P. Anschutz, F. Jorissen, G. Chaillou, R. Abu-Zied, C. Fontanier, Recent turbidite deposition in the eastern Atlantic: Early diagenesis and biotic recovery, Journal of Marine Research 60 (2002). https://elischolar.library.yale.edu/journal_of_marine_research/2455.

[53] M. Gaudin, T. Mulder, P. Cirac, S. Berné, P. Imbert, Past and present sedimentary activity in the Capbreton Canyon, southern Bay of Biscay, Geo-Mar Lett 26 (2006) 331–345. https://doi.org/10.1007/s00367-006-0043-1.

[54] D. Cossa, X. Durrieu de Madron, J. Schäfer, L. Lanceleur, S. Guédron, R. Buscail, B. Thomas, S. Castelle, J.-J. Naudin, The open sea as the main source of methylmercury in the water column of the Gulf of Lions (Northwestern Mediterranean margin), Geochimica et Cosmochimica Acta 199 (2017) 222–237. https://doi.org/10.1016/j.gca.2016.11.037.

[55] K.L. Bowman, C.R. Hammerschmidt, C.H. Lamborg, G. Swarr, Mercury in the North Atlantic Ocean: The U.S. GEOTRACES zonal and meridional sections, Deep Sea Research Part II: Topical Studies in Oceanography C (2015) 251–261. https://doi.org/10.1016/j.dsr2.2014.07.004.

[56] D. Cossa, L.-E. Heimburger, F.F. Perez, M.I. Garcia-Ibanez, J.E. Sonke, H. Planquette, P. Lherminier, J. Boutorh, M. Cheize, J.L.M. Barraqueta, R. Shelley, G. Sarthou, Mercury distribution and transport in the North Atlantic Ocean along the GEOTRACES-GA01 transect, Biogeosciences 15 (2018) 2309–2323. https://doi.org/10.5194/bg-15-2309-2018.

[57] J. Kotnik, M. Horvat, E. Tessier, N. Ogrinc, M. Monperrus, D. Amouroux, V. Fajon, D. Gibičar, S. Žižek, F. Sprovieri, N. Pirrone, Mercury speciation in surface and deep waters of the Mediterranean Sea, Marine Chemistry 107 (2007) 13–30. https://doi.org/10.1016/j.marchem.2007.02.012.

[58] D. Cossa, J.-M. Martin, J. Sanjuan, Dimethylmercury formation in the Alboran Sea, Marine Pollution Bulletin 28 (1994) 381–384. https://doi.org/10.1016/0025-326X(94)90276-3.

[59] R.P. Mason, W.F. Fitzgerald, Alkylmercury species in the equatorial Pacific, Nature 347 (1990) 457–459. https://doi.org/10.1038/347457a0.

[60] R.P. Mason, K.A. Sullivan, The distribution and speciation of mercury in the South and equatorial Atlantic, Deep Sea Research Part II: Topical Studies in Oceanography 46 (1999) 937–956. https://doi.org/10.1016/S0967-0645(99)00010-7.

[61] M. Horvat, J. Kotnik, M. Logar, V. Fajon, T. Zvonarić, N. Pirrone, Speciation of mercury in surface and deep-sea waters in the Mediterranean Sea, Atmospheric Environment 37 (2003) 93–108. https://doi.org/10.1016/S1352-2310(03)00249-8.

[62] J. Kotnik, M. Horvat, E. Begu, Y. Shlyapnikov, F. Sprovieri, N. Pirrone, Dissolved gaseous mercury (DGM) in the Mediterranean Sea: Spatial and temporal trends, Marine Chemistry 193 (2017) 8–19. https://doi.org/10.1016/j.marchem.2017.03.002.

[63] F. Azam, Microbial Control of Oceanic Carbon Flux: The Plot Thickens, (1998) 694–696. https://doi.org/10.1126/science.280.5364.694.

[64] C.T. Driscoll, C.Y. Chen, C.R. Hammerschmidt, R.P. Mason, C.C. Gilmour, E.M. Sunderland, B.K. Greenfield, K.L. Buckman, C.H. Lamborg, Nutrient supply and mercury dynamics in marine ecosystems: A conceptual model, Environmental Research 119 (2012) 118–131. https://doi.org/10.1016/j.envres.2012.05.002.

[65] L. Whalin, E.-H. Kim, R. Mason, Factors influencing the oxidation, reduction, methylation and demethylation of mercury species in coastal waters, Marine Chemistry 107 (2007) 278–294. https://doi.org/10.1016/j.marchem.2007.04.002.

[66] H. Luo, Q. Cheng, X. Pan, Photochemical behaviors of mercury (Hg) species in aquatic systems: A systematic review on reaction process, mechanism, and influencing factor, Science of The Total Environment 720 (2020) 137540. https://doi.org/10.1016/j.scitotenv.2020.137540.

[67] J. Kuss, N. Wasmund, G. Nausch, M. Labrenz, Mercury Emission by the Baltic Sea: A Consequence of Cyanobacterial Activity, Photochemistry, And Low-Light Mercury Transformation, Environ. Sci. Technol. 49 (2015) 11449–11457. https://doi.org/10.1021/acs.est.5b02204.

[68] S.D. Siciliano, N.J. O'Driscoll, D.R.S. Lean, Microbial reduction and oxidation of mercury in freshwater lakes, Environ Sci Technol 36 (2002) 3064–3068. https://doi.org/10.1021/es010774v.

[69] E. Lanzillotta, C. Ceccarini, R. Ferrara, F. Dini, F.P. Frontini, R. Banchetti, Importance of the biogenic organic matter in photo-formation of dissolved gaseous mercury in a culture of the marine diatom Chaetoceros sp, Sci Total Environ 318 (2004) 211–221. https://doi.org/10.1016/S0048-9697(03)00400-5.

[70] S. Oh, M.-K. Kim, Y.-M. Lee, K.-D. Zoh, Effect of Abiotic and Biotic Factors on the Photo-Induced Production of Dissolved Gaseous Mercury, Water Air Soil Pollut 220 (2011) 353–363. https://doi.org/10.1007/s11270-011-0759-z.

[71] R.P. Mason, F.M.M. Morel, H.F. Hemond, The role of microorganisms in elemental mercury formation in natural waters, Water Air Soil Pollut 80 (1995) 775–787. https://doi.org/10.1007/BF01189729.

[72] J.M. Diaz, C.M. Hansel, B.M. Voelker, C.M. Mendes, P.F. Andeer, T. Zhang, Widespread Production of Extracellular Superoxide by Heterotrophic Bacteria, Science 340 (2013) 1223–1226. https://doi.org/10.1126/science.1237331.

[73] K.M. Sutherland, A. Coe, R.J. Gast, S. Plummer, C.P. Suffridge, J.M. Diaz, J.S. Bowman, S.D. Wankel, C.M. Hansel, Extracellular superoxide production by key microbes in the global ocean, Limnology and Oceanography 64 (2019) 2679–2693. https://doi.org/10.1002/lno.11247.

[74] X. Zhang, Y. Guo, G. Liu, Y. Liu, J. Shi, L. Hu, L. Zhao, Y. Li, Y. Yin, Y. Cai, G. Jiang, Superoxide-Mediated Extracellular Mercury Reduction by Aerobic Marine Bacterium Alteromonas sp. KD01, Environ. Sci. Technol. (2023). https://doi.org/10.1021/acs.est.3c04777.

[75] D.S. Grégoire, A.J. Poulain, A little bit of light goes a long way: the role of phototrophs on mercury cycling, Metallomics 6 (2014) 396–407. https://doi.org/10.1039/c3mt00312d.

[76] D.S. Grégoire, A.J. Poulain, A physiological role for HgII during phototrophic growth, Nature Geosci 9 (2016) 121–125. https://doi.org/10.1038/ngeo2629.

[77] J.P. Kim, W.F. Fitzgerald, Sea-air partitioning of mercury in the equatorial pacific ocean, Science 231 (1986) 1131–1133. https://doi.org/10.1126/science.231.4742.1131.

[78] X. Liang, H. Zhong, A. Johs, P. Lei, J. Zhang, N. Taş, L. Zhang, L. Zhao, N. Zhu, X. Yin, L. Wang, E.Y. Zeng, Y. Gao, J. Zhao, D.A. Pelletier, E.M. Pierce, B. Gu, Light-independent phytoplankton degradation and detoxification of methylmercury in water, Nat Water (2023) 1–11. https://doi.org/10.1038/s44221-023-00117-1.

[79] R. Bridou, M. Monperrus, P.R. Gonzalez, R. Guyoneaud, D. Amouroux, Simultaneous determination of mercury methylation and demethylation capacities of various sulfate-reducing bacteria using species-specific isotopic tracers, Environmental Toxicology and Chemistry 30 (2011) 337–344. https://doi.org/10.1002/etc.395.

[80] H. Lin, D.B. Ascher, Y. Myung, C.H. Lamborg, S.J. Hallam, C.M. Gionfriddo, K.E. Holt, J.W. Moreau, Mercury methylation by metabolically versatile and cosmopolitan marine bacteria, ISME J 15 (2021) 1810–1825. https://doi.org/10.1038/s41396-020-00889-4.

706 [81] M. Podar, C.C. Gilmour, C.C. Brandt, A. Soren, S.D. Brown, B.R. Crable, A.V. Palumbo, A.C.
707 Somenahally, D.A. Elias, Global prevalence and distribution of genes and microorganisms
708 involved in mercury methylation, Sci Adv 1 (2015) e1500675.
709 https://doi.org/10.1126/sciadv.1500675.

710 [82] R.P. Mason, A.L. Choi, W.F. Fitzgerald, C.R. Hammerschmidt, C.H. Lamborg, A.L. Soerensen, E.M.
711 Sunderland, Mercury biogeochemical cycling in the ocean and policy implications, Environmental
712 Research 119 (2012) 101–117. https://doi.org/10.1016/j.envres.2012.03.013.

713 [83] C.C. Gilmour, E.A. Henry, R. Mitchell, Sulfate stimulation of mercury methylation in freshwater
714 sediments, Environ. Sci. Technol. 26 (1992) 2281–2287. https://doi.org/10.1021/es00035a029.

715 [84] D. Bianchi, T.S. Weber, R. Kiko, C. Deutsch, Global niche of marine anaerobic metabolisms
716 expanded by particle microenvironments, Nature Geosci 11 (2018) 263–268.
717 https://doi.org/10.1038/s41561-018-0081-0.

718 [85] J. West, A.M. Graham, V. Liem-Nguyen, S. Jonsson, Dimethylmercury Degradation by Dissolved
719 Sulfide and Mackinawite, Environ. Sci. Technol. (2020). https://doi.org/10.1021/acs.est.0c04134.

720 [86] K.H. Coale, W.A. Heim, J. Negrey, P. Weiss-Penzias, D. Fernandez, A. Olson, H. Chiswell, A.
721 Byington, A. Bonnema, S. Martenuk, A. Newman, C. Beebe, C. Till, The distribution and speciation
722 of mercury in the California current: Implications for mercury transport via fog to land, Deep Sea
723 Research Part II: Topical Studies in Oceanography 151 (2018) 77–88.
724 https://doi.org/10.1016/j.dsr2.2018.05.012.

725 [87] H.M. Adams, X. Cui, C.H. Lamborg, A.T. Schartup, Dimethylmercury as a Source of
726 Monomethylmercury in a Highly Productive Upwelling System, Environ. Sci. Technol. (2024).
727 https://doi.org/10.1021/acs.est.4c01112.

728 [88] C.H. Conaway, F.J. Black, M. Gault-Ringold, J.T. Pennington, F.P. Chavez, A.R. Flegal,
729 Dimethylmercury in coastal upwelling waters, Monterey Bay, California, Environ Sci Technol 43
730 (2009) 1305–1309. https://doi.org/10.1021/es802705t.

731 [89] S.G. Kohler, L.-E. Heimbürger-Boavida, M.V. Petrova, M.G. Digernes, N. Sanchez, A. Dufour, A.
732 Simić, K. Ndungu, M.V. Ardelan, Arctic Ocean's wintertime mercury concentrations limited by
733 seasonal loss on the shelf, Nat. Geosci. (2022) 1–6. https://doi.org/10.1038/s41561-022-00986-
734 3.

735 [90] P.A. Baya, M. Gosselin, I. Lehnherr, V.L. St.Louis, H. Hintelmann, Determination of
736 Monomethylmercury and Dimethylmercury in the Arctic Marine Boundary Layer, Environ. Sci.
737 Technol. 49 (2015) 223–232. https://doi.org/10.1021/es502601z.

738 [91] J. West, D. Babi, A. Azaroff, S. Jonsson, Dimethylmercury in natural waters—analytical and
739 experimental considerations, Limnology and Oceanography: Methods 21 (2023) 837–846.
740 https://doi.org/10.1002/lom3.10586.

741 [92] S.G. Kohler, L.-E. Heimbürger-Boavida, P. Assmy, O. Müller, S. Thiele, M.G. Digernes, K. Ndungu,
742 M.V. Ardelan, Biotic transformation of methylmercury at the onset of the Arctic spring bloom,
743 Progress in Oceanography 222 (2024) 103224. https://doi.org/10.1016/j.pocean.2024.103224.

744

745 # TOC Graphic